

Cu-doped ZnO/Ag/CuO heterostructure: superior photocatalysis and charge transfer

Abbay Gebretsadik,^a Bontu Kefale,^a Chaluma Sori,^a Dereje Tsegaye,^a H C Ananda Murthy *^{b†} and Buzuayehu Abebe *^a

^aDepartment of Applied Chemistry, Adama Science and Technology University, 1888, Adama, Ethiopia

^bSchool of Applied Sciences, Papua New Guinea University of Technology, Lae, Morobe Province, 411, Papua New Guinea.

[†]Department of Prosthodontics, Saveetha Dental College & Hospital, Saveetha Institute of Medical and Technical Science (SIMATS), Saveetha University, Chennai 600077, Tamil Nadu, Indi.

Figures

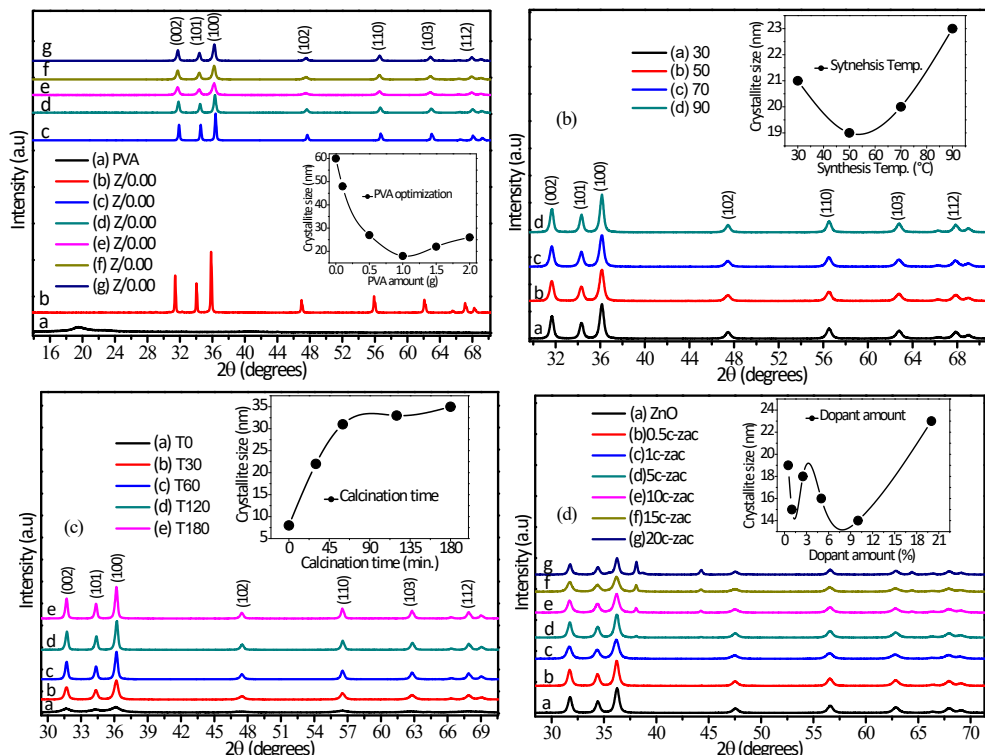


Fig. S1. ZnO crystallite size optimization using the X-ray diffraction pattern: (a) the effects of PVA amount, (b) synthesis temperature, (c) Calcination time, (d) dopant amount were studied and optimized. The 1.00 g of PVA, 50 °C synthesis temperature, and 1 hour calcination time were obtained to be the optima.

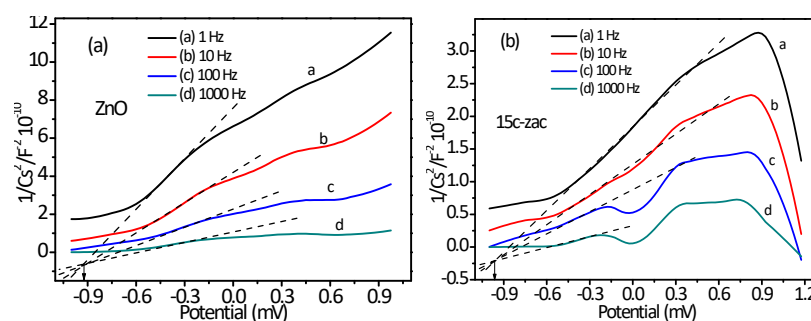


Fig. S2. (a and b) Schottky plots of ZnO NPs and c-zac heterostructure, respectively.

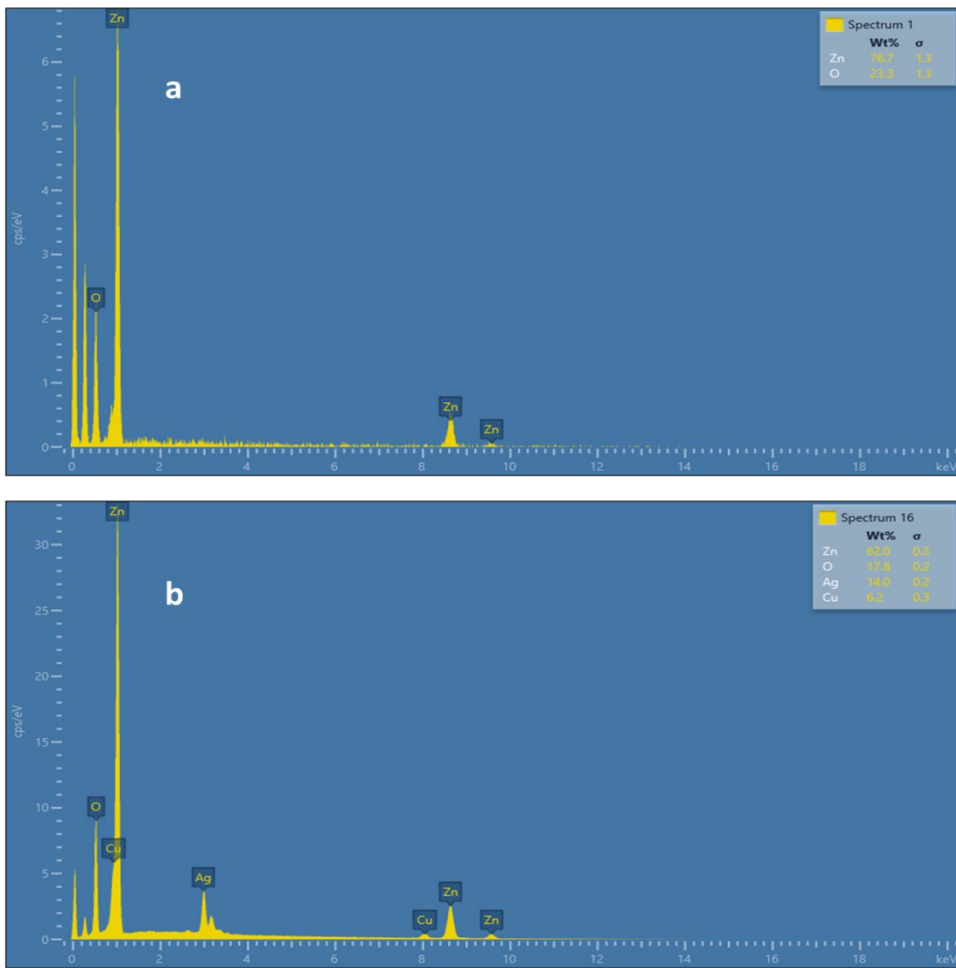


Fig. S3. EDX elemental and compositional analysis for (a) ZnO NPs and (b) c-zac heterostructure.

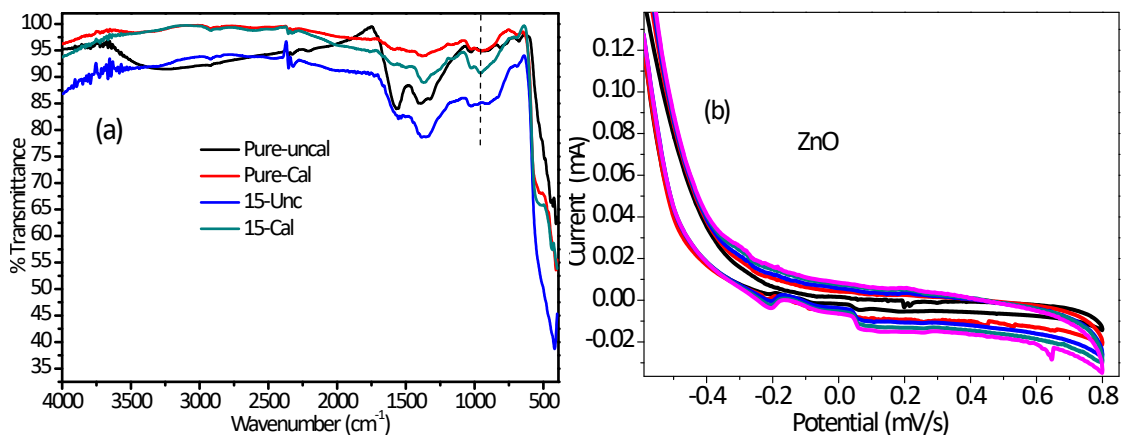


Fig. S4. Functional group and metal-oxygen bond properties of uncalcined and calcined ZnO NPs and the c-zac heterostructure. There is a higher wavenumber shift for calcined NPs compared to uncalcined NPs and heterostructure, which is due to the metal-oxygen bond stiffness. The distinctive peak was detected at 950 cm^{-1} on the c-zac heterostructure, which is from doped CuO, (b) ZnO NP electrochemical analysis using the cyclic voltammetry.

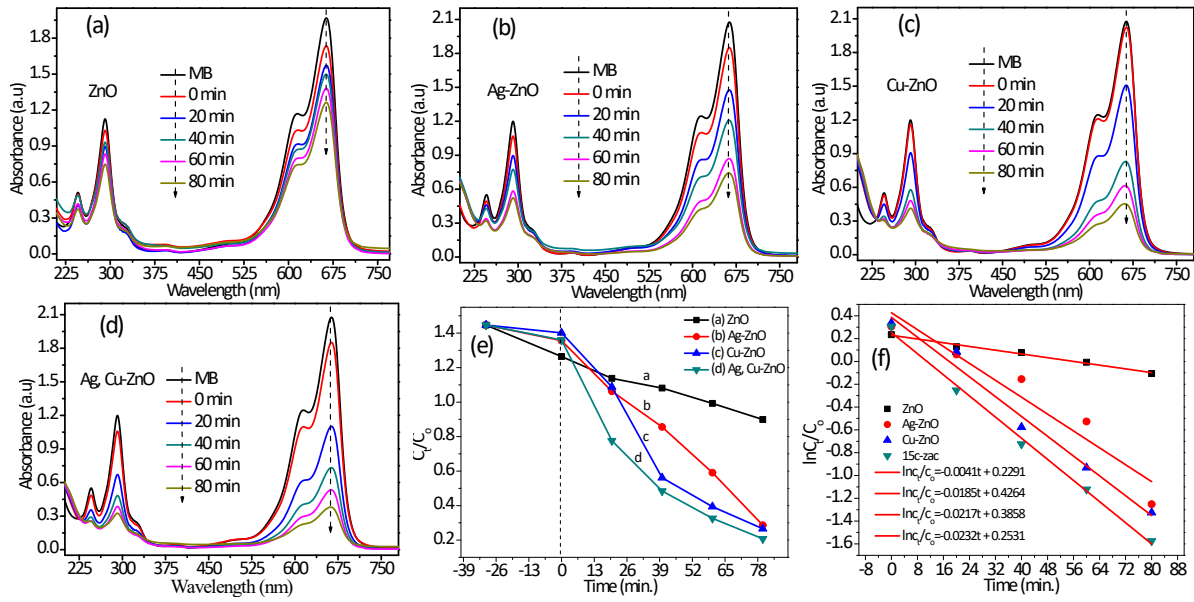


Fig. S5. absorbance vs. wavelength plots of (a) ZnO NPs, (b) Ag-ZnO, (c) Cu-ZnO, and (d) c-zac heterostructure at an initial MB concentration of 10 ppm and a catalyst amount of 20 mg, (e and f) the C_t/C_0 and $\ln(C_t/C_0)$ versus time plots of the NPs and heterostructures. The c-zac heterostructure has greater photocatalytic performance due to its improved optoelectric properties and synergistic effect.

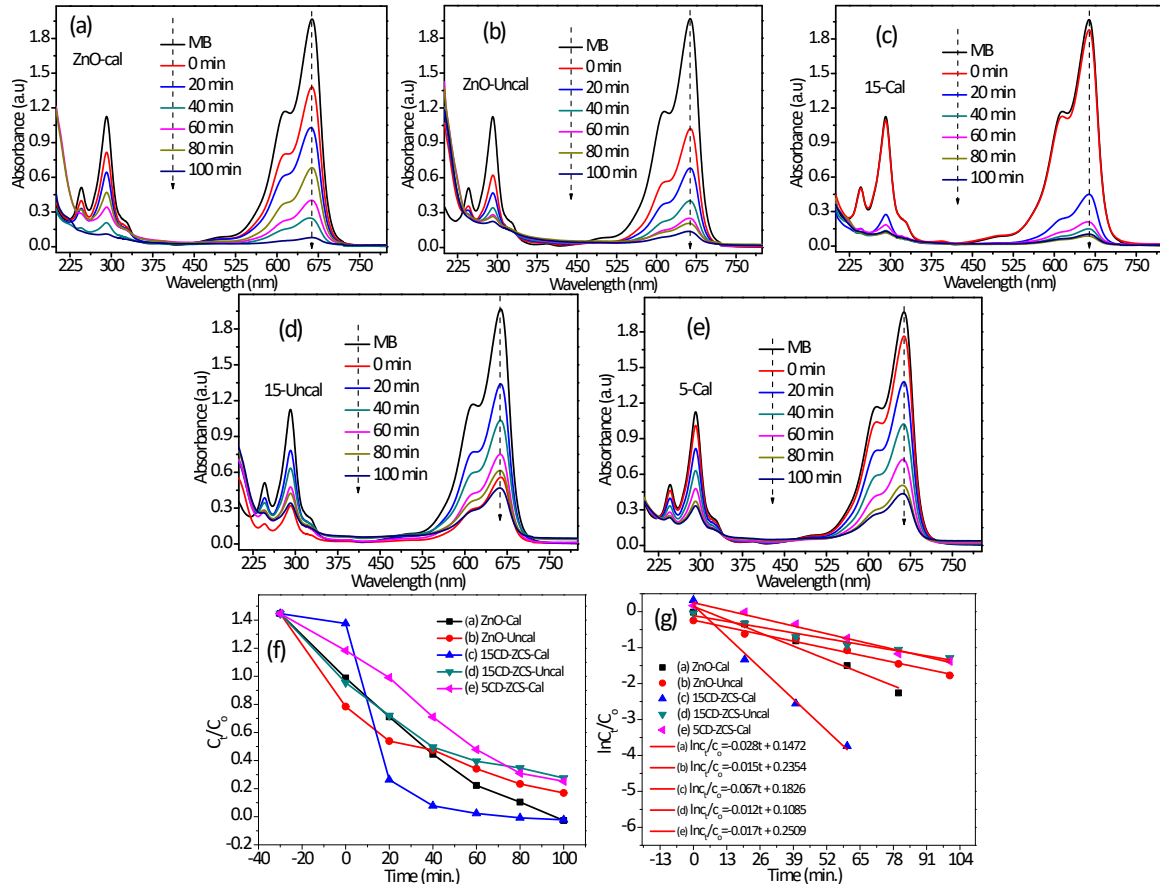


Fig. S6. The absorbance vs. wavelength plots of calcined and uncalcined (a and b) ZnO NPs, (c and d) 15c-zac, (e) calcined 5c-zac heterostructures at an initial MB concentration of 10 ppm, a catalyst amount of 20 mg, and a solution pH of 9, (f and g) C_t/C_0 and $\ln(C_t/C_0)$ versus time plots of the NPs and heterostructures. A catalyst amount of 20 mg has greater photocatalytic performance. The calcined NPs and heterostructure showed greater photocatalytic performance, probably due to the greater crystallinity effects. However, the 15c-zac heterostructure has greater performance compared to both ZnO NPs and the 5c-zac heterostructure.

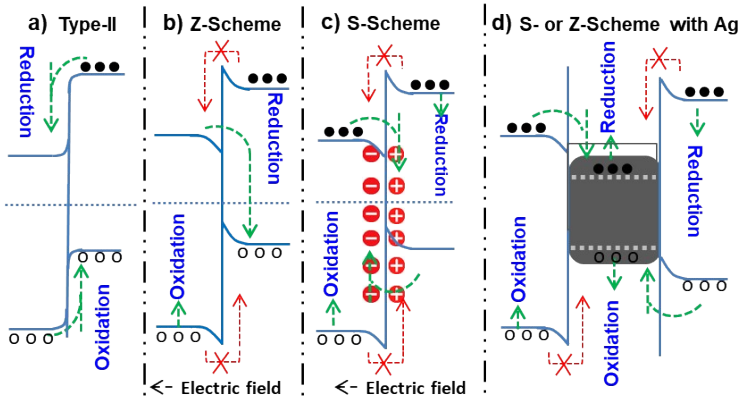


Fig. S7. The possible (a) type-II (staggered), (b) Z-Scheme, (c) S-Scheme charge transfer mechanisms between CuO and ZnO, (d) Z- or/and S-scheme mechanisms in the presence of silver as a mediator. In Z- and S-scheme mechanisms, electrons and holes with less thermodynamic energy are lost by recombination and quenching. The silver decreases recombination and quenching problems as well as extends visible light absorption.